Forming Magnetosome-Like Nanoparticles in Mammalian Cells for Molecular MRI

Donna E. Goldhawk, Neil Gelman, R. Terry Thompson, and Frank S. Prato

1 Introduction

As an understanding of the molecular basis of disease becomes crucial for treatment and diagnosis, there is a growing need to noninvasively image these processes in preclinical animal models and human clinical trials. However, in order to track molecular activity effectively using current medical imaging platforms, increased sensitivity of detection as well as improved spatial and temporal resolution are needed. With optical imaging technology, such as bioluminescence and fluorescence, the use of reporter genes has been very successful for interrogating molecular activity in cells and very small animal models [1–3]. As optical imaging is limited due to light scatter and attenuation, in vivo reporter gene imaging of larger animals currently relies on nuclear medicine and magnetic resonance (MR) reporter genes. In addition, there is growing evidence that results from small animal imaging cannot be easily translated to humans. This difficulty relates not only to species-specific differences [4, 5] but also to differences in imaging platform, wherein the

D.E. Goldhawk (✉) • F.S. Prato
Imaging Program, Lawson Health Research Institute,
268 Grosvenor Street, London, ON, Canada, N6A 4V2

Medical Biophysics, Western University, London, ON, Canada

Collaborative Graduate Program in Molecular Imaging, Western University,
London, ON, Canada
e-mail: dgoldhawk@lawsonimaging.ca

N. Gelman • R.T. Thompson
Imaging Program, Lawson Health Research Institute,
268 Grosvenor Street, London, ON, Canada, N6A 4V2

Medical Biophysics, Western University, London, ON, Canada

J.W.M. Bulte, M.M.J. Modo (eds.), *Design and Applications of Nanoparticles in Biomedical Imaging*, DOI 10.1007/978-3-319-42169-8_9

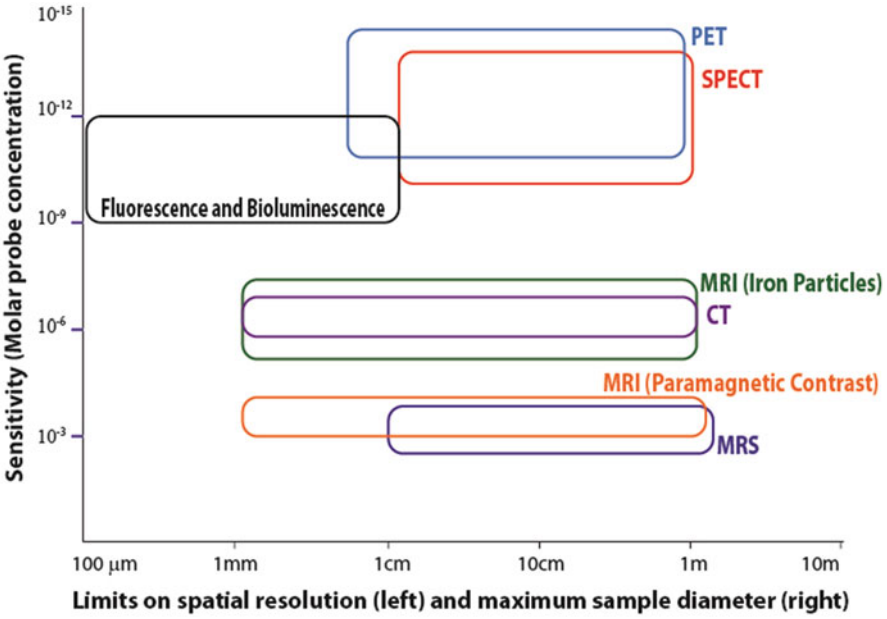

Fig. 1 Comparison of the capability of different large animal and human molecular imaging modalities. The matrix uses a log-log scale to indicate sensitivity on the vertical axis and spatial resolution on the horizontal axis. Maximum resolution corresponds to the left limit on the horizontal axis and maximum sample diameter corresponds to the right limit. The sensitivity range for PET is taken from Meikle et al. [71] and spatial resolution from Moses [6]. The sensitivity for SPECT is also taken from Meikle et al. [71] and spatial resolution is estimated at 1.2 cm; however, this is dependent on collimator choice and distance from collimator to object [72]. For fluorescence and bioluminescence imaging, resolution limit can be higher than the optical wavelength [73], i.e., much better than 100 µm, but decreases very quickly for an object of any thickness. A 1 cm limit for thickness is generous and corresponds to hybrid methods such as photoacoustic imaging [74]. For MRI with paramagnetic contrast agents, 1 mm^3 resolution at 3 T is easily achievable, with sample size being limited by available magnet bore [75]. For MRI with iron particles, refer to the section on estimated limits of sensitivity of a MRI reporter gene. For magnetic resonance spectroscopy (MRS), the spatial resolution for ^{31}P, ^{19}F, ^{23}Na, or ^{1}H (from non-water protons) is limited to approximately 1 cm due to gyromagnetic ratio and/or concentration of the isotope [76]. The values for CT were taken from Gore et al. [76]

resolution of small animal imaging does not match the scale of large animal/human systems [6]. There is also evidence that large animal studies (e.g., in dogs, pigs) are more indicative of the human condition [7] and will improve translational efficiency. To image on this clinical scale, only nuclear medicine reporter genes currently offer the needed sensitivity (comparable to optical); however, the spatial resolution is limited to about 64 mm^3 (Fig. 1). To capitalize on the superb spatial (approximately 1 mm^3 on clinical scanners) and temporal resolution of magnetic resonance imaging (MRI), further development of a magnetite-based MR reporter gene would substantially improve molecular imaging in both small and large animals, providing a route for seamless translation of medical imaging technology to human care.

The idea of using magnetotactic bacterial genes as noninvasive reporters of cellular activity for molecular MRI has recently been put forward [8–10]. Magnetotactic bacteria form magnetosomes [11, 12], membrane-enclosed iron biominerals that respond to the earth's magnetic field and enable magnetotaxis. With these attributes, the motile microaerophilic bacteria may navigate toward their preferred oxic-anoxic zones in aquatic sediments [13]. Magnetosomes are also similar in size and magnetic properties [14] to superparamagnetic iron oxide (SPIO) nanoparticles. While the latter have been used successfully to track cells in both research and clinical settings [15–18], within the genetic determinants of magnetosome synthesis is an opportunity to specify MR contrast as a direct response of select gene expression.

Approximately 20 years ago, a few reports were published about genes related to the magnetic properties of species of *Alphaproteobacteria* [19, 20]; although, it is only in the last decade that a clearer definition of the magnetosome and its constituent proteins has emerged [21]. The magnetosome is formed by a group of nonessential genes, suggesting that this bacterial structure is dispensable and confers an auxiliary function to the cell, i.e., magnetotaxis. When present, the magnetosome comprises an iron biomineral that is compartmentalized within a specialized lipid bilayer, protecting the cell from iron toxicity and confining the biomineral to a defined subcellular location. As detailed below, the magnetosome membrane contains a number of proteins that direct its location and crystal composition, size, and shape. In short, the magnetosome is an ideal structure by which cellular and molecular MRI may be refined.

Recent progress in defining the magnetosome in molecular terms provides an opportunity to further develop genetically engineered, MR contrast for effective molecular MRI [22, 23]. Such a tool would address the critical need to identify molecular activities that define the early stages of disease progression, ahead of the irreversible damage to tissue that leads to chronic illness. This is where the true strength of noninvasive reporter gene expression lies. The ability to detect transcription factor activity that prompts disease-related changes in gene expression is the key to understanding many, if not most medical conditions, including cancer [24, 25], inflammation [26, 27], and the fibrosis that leads to heart disease [28, 29]. Effective use of MRI reporter gene expression vectors, which create and strictly regulate magnetosome-like particles in mammalian cells, could provide the spatial and temporal information necessary to track disease processes and influence healthcare management and rate of cure.

This chapter describes recent progress in understanding how the magnetosome is formed in bacteria and how these mechanisms may be adapted to the formation of magnetosome-like particles in mammalian cells. From an MR imaging perspective, the expression of magnetotactic bacterial genes *magA* and *mms6* in mammalian cells provides the basis for a discussion on future development of MR detection methods, needed to optimize the use of gene-based MR contrast and its application in diagnostic medical imaging.

2 Design

2.1 Formation of Magnetosome-Like Nanoparticles in Mammalian Cells

To date, reports assessing the function of magnetotactic bacterial protein expression in mammalian cells have centered around MagA and to a lesser degree Mms6. To give perspective to this body of work, we first describe the bacterial magnetosome compartment that has inspired this approach to the development of gene-based MR contrast. Based on the current understanding of magnetosome formation, we then categorize the genes identified in terms of essential versus auxiliary function(s). Finally, we highlight useful features for the design of magnetosome-like nanoparticles in mammalian cells before discussing their applications in MRI.

Magnetosomes are subcellular structures encoded by approximately 30 genes, many of which reside on a conserved magnetosome genomic island (MAI), are not essential for survival, and are not expressed when bacterial cells are grown in nutrient-rich broth and have little need for magnetotaxis [30]. Deletion of either the MAI or one of its gene clusters, the *mamAB* operon [31], results in the loss of magnetosome formation [32] and underlines the important regulatory role of select magnetosome genes. As the structure and activity of individual magnetosome-associated proteins have been reported, models of magnetosome assembly have been proposed [12, 33] and refined. A recent model outlines four main stages: (a) vesicle formation, (b) magnetosome protein sorting, (c) cytoskeletal attachment, and (d) biomineralization [12]. Figure 2 depicts this process and identifies putative roles of select genes in membrane biogenesis and recruitment of proteins that facilitate vesicle formation, organization of magnetosomes into a chain, initiation of biomineralization, and definition of the mature crystal structure. Over the last 10 years, much evidence has accumulated indicating that magnetosome formation is an ordered process and relies on specific protein interactions. As the understanding of these protein activities becomes clearer, so does the means by which this technology can be adapted for medical imaging, among other applications. Here, we provide an MR imaging perspective and assess the genes involved in magnetosome synthesis in terms of essential versus auxiliary functions. With this categorization, we draw on one of the best cellular models of biomineralization to provide a context for continued development of the next stage of mammalian cell tracking and reporter gene expression for MRI.

2.2 Formation of a Magnetosome-Like Vesicle

All organisms require iron and carefully manage its redox chemistry through an elaborate set of regulatory mechanisms [22, 34]. Although iron is an essential cofactor for the function of many proteins, in general iron biominerals are not. Where they occur

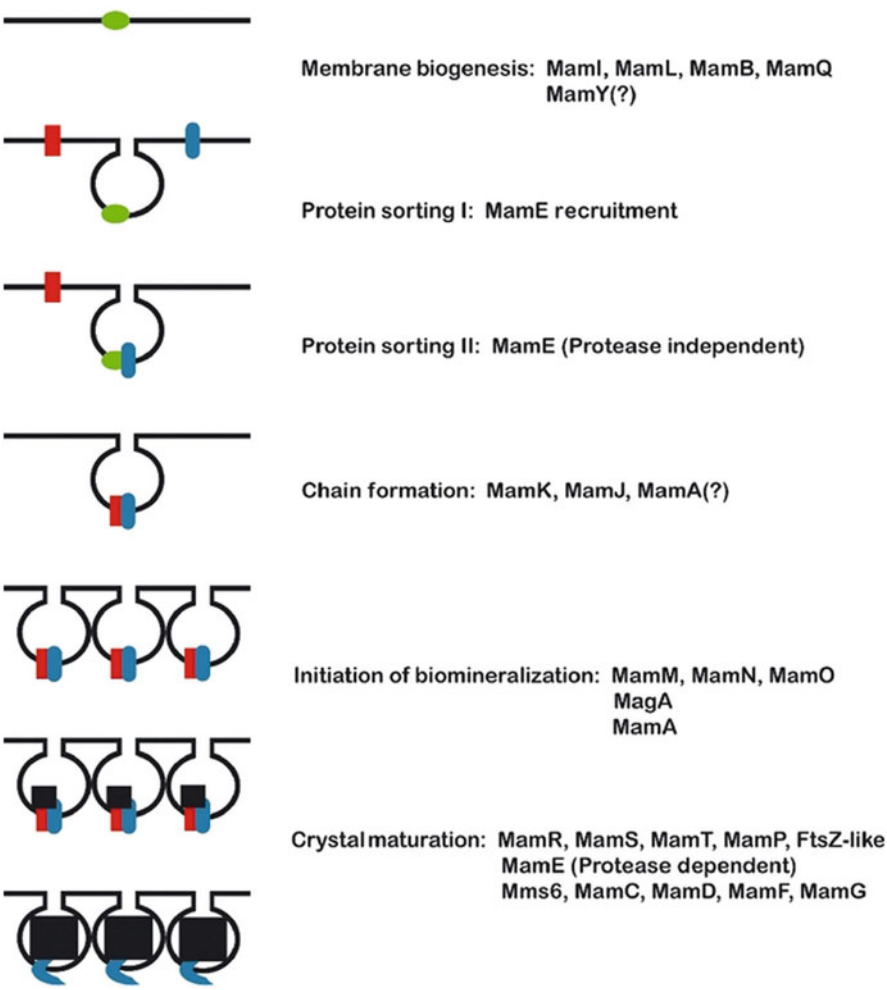

Fig. 2 Hypothetical model of magnetosome formation. Partial characterization of magnetotactic bacterial genes, particularly from the *Alphaproteobacteria*, provides further support for protein-directed assembly of the magnetosome. Largely based on genes located on the magnetosome genomic island found in multiple species of magnetotactic bacteria, the depicted stages of magnetosome synthesis include magnetosome membrane biogenesis through recruitment of the needed proteins for vesicle formation, arrangement of these magnetosome vesicles into a chain, followed by initiation and maturation of the iron biomineral. In the latter stage, factors that control crystal size and morphology vary among different classes of magnetotactic bacteria. Reproduced with permission from Ref. [12]

naturally, even as stored in ferritin, the iron biomineral is invariably sequestered to protect the cell from its potential toxicity. Accordingly, in magnetotactic bacteria the membrane-enclosed vesicle that will sequester an iron biomineral is recognized as the first step in magnetosome synthesis. Thus, in the design of magnetosome-like

nanoparticles for mammalian cell tracking, appropriate compartmentalization of the iron biomineral is an essential step and may be refined by examining the magnetotactic bacterial protein(s) that specify the magnetosome compartment.

Biosynthesis of the magnetosome membrane was originally identified as an invagination of the inner plasma membrane in *Magnetospirillum magneticum* species AMB-1 [35]. However, a broader examination of magnetotactic bacteria reveals multiple arrangements of magnetosomes [13] and raises the possibility that not all magnetosomes are, or remain, associated with the plasma membrane [12]. The independent existence of magnetosome vesicles is most likely defined by the proteins that sort to this location and specify vesicle function. Key proteins involved in this process are encoded by genes located within a DNA cluster that is widespread among classes of magnetotactic bacteria [36], the *mamAB* operon [31], and whose expression is coordinately regulated. Of these genes, individual deletion of *mamI*, *mamL*, *mamQ*, and *mamB* results in no magnetosome membrane; however, none of these genes alone is sufficient for its formation. Interestingly, MamI and MamL are small proteins unique to magnetotactic bacteria [32] and MamL is not found in greigite-producing *Deltaproteobacteria*, suggesting a unique role for MamL in magnetite-producing *Proteobacteria* [37].

It remains to be seen what combination of genes may be needed for optimal expression of a magnetosome-like particle in mammalian cells. The likely subset of magnetosome genes will depend on the functionality desired but will probably possess a root structure that provides the scaffold for compartmentalization of the iron biomineral. With this scaffold, the recruitment of specific genes will not only be feasible but also programmable, delivering the type of MR signal that is prescribed by selective expression of magnetosome protein (see reporter gene expression below). The nature of the required protein sorting to the magnetosome membrane is still poorly defined; however, several studies substantiate a role for protein-protein interactions [38]. For example, MamB interacts with other magnetosome-associated membrane proteins, MamM and MamE [39]. The important role of MamE in recruiting additional magnetosome proteins to the membrane for crystal formation has recently emerged [40]. Deletion of *mamE* results in a nonmagnetic mutant that can nevertheless form empty magnetosome vesicles [12]. It appears that MamE provides a link to biomineralization partly through its interactions with MamI and MamB [32]. These interactions also likely contribute to the correct orientation of magnetosome proteins in the membrane so that crystallization is appropriately initiated within the vesicle. Separate functional domains of MamE have also been partially characterized [40]. Putative serine protease and heme-binding activity is associated with the N-terminal domain while protease-independent function in the C-terminal domain may be principally involved in recruiting magnetosome membrane protein(s). In some species of *Deltaproteobacteria*, the N- and C-terminal domains of MamE are encoded by separate genes [37], suggesting that strategies for streamlining mammalian expression of magnetosome genes may include the expression of functional gene fragments.

2.3 Formation of a Magnetosome-Like Biomineral

Critical magnetosome genes for iron biomineralization include *mamE, mamO, mamM,* and perhaps *mamN*. These genes from the *mamAB* operon appear to facilitate the initiation of iron biomineralization but are not sufficient for obtaining the final size and shape of the desired crystal structure [12]. The distinction between early and late events in biomineralization again reinforces the ordered nature of this process (Fig. 2). As a consequence, the optimal expression of magnetosome-like nanoparticles in mammalian cells will benefit from a clearer understanding of the temporal relationship between the required biomineralization activities. Once initiated, the controlled expression of magnetosome genes in the correct sequence will provide landmarks by which changes in MR contrast may be measured and correlated to discrete cellular activities. Eventually, we envision this strategy would include complementary expression systems that when activated create a more refined magnetosome-like particle than was possible when individually expressed.

Based on the study of magnetotactic bacteria harboring deletions of select magnetosome genes, attempts are being made to understand which genes are essential to the basic magnetosome structure and which genes have more auxiliary roles, for example in defining the location and configuration of magnetosomes within the cell or in specifying the nature of the biomineral. Many of the MAI genes involved in crystal maturation have such auxiliary functions; their absence mitigates but does not abrogate magnetosome formation. The entire *mamCGDF* operon encodes some of the most abundant magnetosome proteins that are nevertheless not essential for the formation of a more rudimentary particle [41]. Likewise, the *mms6* operon is directly involved in iron biomineralization and its absence diminishes the process but does not completely interrupt it [32]. In addition, several more proteins encoded within the *mamAB* operon appear to have a role in the final stage(s) of iron biomineralization and could be excluded without interrupting the synthesis of the core structure. The presence of all these MAI genes provides a powerful argument for the feasibility of producing a magnetosome-like particle in mammalian cells using a subset of magnetotactic bacterial genes. Furthermore, within this subset of gene products are protein domains that may function similarly to known mammalian proteins (or their functional domains) and could be used in combination with unique bacterial magnetosome proteins. Zeytuni et al. have described the similarity between MamM, a putative cation diffusion facilitator (CDF) protein, and a mammalian member of the CDF superfamily implicated in type II diabetes [42]. They generated mutant MamM to model CDF polymorphisms present in human disease and the manner in which select mutations influence cation transport, in this case using the change(s) in magnetosome biomineralization to monitor the change in CDF function. This work establishes the broad utility of magnetosome synthesis for biomedical research, with important ramifications for the development of gene-based MR contrast using magnetosome-like nanoparticles.

There are homologues to several of the genes on the *mamAB* operon in other classes of magnetotactic bacteria. Species of *Deltaproteobacteria* that produce

bullet-shaped crystals of greigite and/or magnetite have homologues of *mamI*, *mamL*, and *mamM* [37]. By comparing genomes, Lefèvre et al. have suggested that *mamA*, *mamB*, *mamE*, *mamK*, *mamO*, *mamP*, and *mamQ* are involved in the synthesis of all types of magnetosomes, whether greigite or magnetite. In addition, *mamI*, *mamL*, and *mamM* may be specific to magnetite crystals while a distinct set of genes, termed *magnetosome-associated Deltaproteobacteria* (*mad*) genes, specifies greigite biomineralization. These interesting projections are largely based on nucleotide and amino acid sequence alignments, which provide a useful roadmap for understanding magnetosome synthesis but will require experimental validation.

The best studied magnetosomes typically contain magnetite (Fe_3O_4) in a cubo-octahedral crystal [43]. However, the dynamic nature of magnetosome synthesis includes different types of biominerals, varying in composition (e.g., greigite, Fe_3S_4) [13, 21], crystal structure, and size [37]. For MRI, the ideal size of a magnetosome-like particle in mammalian cells may be smaller than that needed to establish a single magnetic domain. While larger biominerals might be required for MR-guided movement or thermal ablation [44], many applications such as magnetic particle imaging (MPI, discussed below) place constraints on biomineral size and composition. Hence, not every aspect of the bacterial magnetosome should necessarily be reproduced for mammalian cell tracking. By regulating the formation of a magnetosome-like particle in mammalian cells, we could draw on select features of the nanoparticle and avoid functions that are not indicated for a given application, such as unwanted heating or movement that might disrupt tissue at higher field strengths. Both thermal and kinetic properties may depend on the arrangement of magnetosome(-like) particles within the cell. Since MamJ and MamK have principle roles in chain formation, their optional expression may provide added versatility and would certainly streamline the number of genes required to create magnetosome-like particles in mammalian cells.

Recently, Kolinko et al. described the stepwise expression of MAI gene clusters that closely recapitulated the magnetosome structure in a previously nonmagnetic bacterium, *Rhodospirillum rubrum* [45]. This report provides further evidence that a subset of magnetosome genes may be used to impart magnetic properties and that potentially all types of cells, from bacteria to mammals, may accommodate this nanoparticle without cytotoxic consequences.

3 Applications

3.1 MagA-Derived Iron-Labeling and MR Contrast

A putative iron transport protein, MagA, has been cloned from both MS-1 [10] and AMB-1 [8] species of magnetotactic bacteria and shown to increase MR contrast in stably transfected mammalian cells, in response to an iron supplement. Compared to overexpression of a modified form of ferritin, lacking iron response elements to enable continuous expression, MagA-derived MR contrast appears sooner in mouse

tumor xenografts growing subcutaneously from transplanted cells and with greater contrast to noise ratio (CNR) [46]. An in vitro analysis of MR relaxation rates confirmed that iron-supplemented MagA-expressing cells provide significant increases in transverse relaxation rates (R_2*, R_2, and R_2'), with little or no change in longitudinal relaxation [47]. Elemental iron analysis in these cells also correlated an increase in iron content with the increase in transverse relaxation rate and the reversible R_2' component in particular [22].

To better understand the mechanisms of transverse relaxation in MagA-expressing iron-labeled cells, Lee et al. performed nuclear magnetic resonance experiments to study the relationship between R_2 and interecho time (2τ), as assessed with a Carr-Purcell-Meiboom-Gill (CPMG) sequence [48]. The R_2 versus 2τ curves were analyzed using a previously developed numerical model [49] that provided estimates of the so-called spatial correlation length, representing the distance scale of microscopic magnetic field variation. In a model where this magnetic field variation is caused by uniformly magnetized spheres within tissue, they showed that the spatial correlation length is approximately equal to the sphere radius. Using this method, the spatial correlation length estimated by Lee et al. in iron-supplemented, MagA-expressing MDA-MB-435 cells was on the order of 250–450 nm, reasonably consistent with transmission electron micrographs of MagA-expressing 293FT cells [10]. In these micrographs, it should be noted that the size of dense core clusters and the size of individual particles within these clusters (estimated at 3–5 nm [10]) are approximately 100-fold different. If the putative magnetosome-like particle size created in mammalian systems (i.e., dense core clusters) through the expression of a single magnetotactic bacterial gene is comparable to the bacterial magnetosome (~50 nm), then the biomineral structure and magnetic properties are still poorly developed. This is not surprising given the number of MAI genes used by magnetotactic bacteria, especially for growth of the biomineral (Fig. 2). Even the expression of Mms6 alone, a magnetosome protein involved in crystal maturation [50], provided an MR signal and particle size in mammalian cells that was no better than MagA-derived contrast [9]. Taken together, these results and the current understanding of magnetosome synthesis suggest that a combination of genes is likely needed to improve the biomineral structure and MR signal derived from a magnetosome-like particle in mammalian cells.

However rudimentary, MagA and Mms6 expression each provide a baseline MR signal upon which to build. These magnetotactic bacterial genes are compatible with mammalian cell culture models and/or tumor cell biology [46], and in a variety of mammalian systems MagA expression poses no apparent immune or cytotoxic responses [8, 51, 52]. In addition, the feasibility of inducible MagA expression in mouse embryonic stem cells was recently demonstrated using intracranial grafts and 7 T MRI [53]. Despite these proof-of-principle studies, relatively few magnetosome-associated genes have been tested in mammalian cell systems; however, a more thorough examination of these bacterial genes may further augment and refine gene-based MR contrast. The research in mammalian models should also help clarify which magnetotactic bacterial genes are essential for a properly functioning magnetosome and how best to modify this structure for different biotechnological applications.

3.2 Reporter Gene Expression

Collingwood and Davidson have recently reviewed methods of measuring iron biominerals, their localization, and quantification in the cell using synchrotron technology [54]. The authors conclude that the most important thing to understand about the role of iron in neuropathology is not the total concentration of iron or its localization in the cell but rather the interactions between iron and iron-handling protein(s). If correct, then the interactions of magnetosome and mammalian proteins should be invaluable for enhancing the influence of iron biomineral properties on the MRI signal and for identifying distinct MR signatures.

Virtually, all models of magnetosome assembly now incorporate the notion of a protein scaffold, in which sequential addition of proteins that interact generates the molecular structure required for optimal function. The scaffold is like what you find on a construction site when laborers need to work on the roof. If pieces are missing, then you cannot build a structure high enough to complete the job. Similarly, the framework upon which one builds a magnetosome-like nanoparticle in mammalian cells may entail several proteins that do not produce contrast but without which effective MR contrast cannot be achieved. This is an opportunity for reporter gene expression of genes that somehow complement the structure of the iron biomineral, be that proper formation of the magnetosome compartment, arrangement within the cell, composition of the crystal, its shape or size.

3.3 MRI Detection of Iron Metabolism

Perhaps an unexplored benefit of developing methods for detection of gene-based contrast is the potential use of MRI for measuring changes in iron metabolism [22]. In most cell culture models, MagA expression increases the amount of cellular iron, only in response to an extracellular iron supplement [47]. In this way, MagA acts as a beacon indicating a change in the extracellular environment, which may ultimately be a useful diagnostic tool.

For multipotent P19 cells, in which the parental line displays high iron import and export, similar to the iron recycling phenotype of M2 macrophages, the influence of MagA expression modulates iron export but has little effect on iron uptake [51]. Although further studies are needed to delineate the mechanism of MagA function in mammalian cells, there may be a therapeutic role for MagA expression in iron regulation or dysregulation. With the increasing awareness and understanding of inappropriate iron handling in neurological disorders [54], blood disorders [55], and inflammation [28, 56], future cell therapies might benefit from the magnetosome-like particle as a vehicle for removal or delivery of iron.

3.4 Estimated Limits of Sensitivity of MRI Reporter Gene Expression Based on the Magnetosome

Assuming that mammalian cells can eventually be engineered to express a magnetosome-like particle with the same capacity to produce iron biominerals as magnetotactic bacteria, per unit volume, we have estimated the limit of sensitivity of MRI reporter gene expression. We will express this limit as the number of mammalian cells required to produce a change in R_2 (ΔR_2) of 1 s^{-1}. For this calculation, we have used the results of Benoit et al. [57] in which magnetotactic bacteria were imaged within mouse tumors. In this work, the amount of iron per bacterial cell was measured by magnetometry and gave 2.2×10^{-15} g (3.9×10^{-11} μmol Fe) when the bacteria were cultured in the presence of 40 μM ferric malate and 0.64×10^{-15} g (1.15×10^{-11} μmol Fe) when the iron supplement was 40 μM $FeCl_3$. The corresponding R_2 relaxivities reported were 48 s^{-1}/mM and 337 s^{-1}/mM, respectively. Using the latter value, the concentration of iron required to produce a ΔR_2 of 1 s^{-1} is equal to 1 s^{-1}/(337 s^{-1}/mM) ≈ 3 μM. Assuming that mammalian cells could hold approximately 100 times more iron than magnetotactic bacteria, this iron concentration corresponds to a cellular concentration of (3 μmol/L)/($100\times1.15\times10^{-11}$ μmol/cell) = 2.6×10^9 cells/L. For imaging of large animals and humans, one can assume a 1 μL voxel, and hence the number of cells per voxel required to produce a ΔR_2 of 1 s^{-1} would be 2600. In order to extend this estimate to small animal (e.g., mouse) imaging using the same criterion ($\Delta R_2 = 1$ s^{-1}), we must assume similar signal to noise ratio (SNR) as in the large animal case. We note that SNR scales with the volume of tissue (V_T) within the radiofrequency coil as $1/(V_T)^{5/6}$ [58]. For a mouse (20 g) compared to a human (70 kg) this corresponds to a factor of $(3500)^{5/6}$ for an estimate of ~900–1000 cells. Therefore, assuming similar sequence and coil design for mouse and human imaging, the corresponding mouse voxel would be 10^{-3} μL. Hence, the number of cells in this small animal voxel required to produce a ΔR_2 of 1 s^{-1} would be approximately 2600/1000 ~ 3. Based on this calculation, sensitive imaging of relatively few cells could theoretically be achieved by developing MRI reporter gene expression modeled on the magnetosome.

To approach this projection in vivo, mammalian cells expressing a magnetosome-like particle would presumably draw on cellular stores of iron. Typically, this involves the uptake of transferrin-bound iron from the circulation, which is introduced into cells through transferrin receptor-mediated endocytosis [22]. Once internalized, iron homeostasis is tightly regulated by Iron Binding Proteins. Excess iron is stored in ferritin while the labile iron pool provides metal ion cofactor for the immediate needs of the cell. Consistent with this, MagA-derived MR contrast in P19 cells reduces apparent iron export activity, with little or no influence on iron uptake [59]. This finding suggests that intracellular iron may be rerouted for different purposes and in response to magnetotactic bacterial transgene expression.

3.5 Applications in Magnetic Particle Imaging

Particles of maghemite (γ-Fe_2O_3), an oxidized form of magnetite [60], are used exclusively in MPI. The size of these superparamagnetic iron oxide nanoparticles (SPION) is smaller than the iron core needed to hold one magnetic field domain. Consequently, SPION have predominantly fast relaxation rates as the internal magnetization of the iron core rotates in response to an external time-changing magnetic field (Néel relaxation). When the size of an iron biomineral exceeds approximately 25 nm, as is the case for most magnetosomes produced by bacteria, the particle then holds one magnetic field domain and responds to an altered magnetic field, such as used in MPI, primarily by Brownian relaxation. This motion requires the particle itself to rotate in its environment. Since both the iron core and the nonmagnetic outer shell must physically rotate, Brownian relaxation is much slower than Néel relaxation. Thus, in general MPI is optimal (with respect to spatial resolution and SNR) when the iron core of the MPI tracer is just below the transition from Néel to Brownian relaxation [61]. In addition, the dependence of imaging frequency on particle size permits MPI to discriminate SPION of different sizes [62].

Depending on the species, magnetotactic bacteria synthesize magnetosomes that range in size and shape of the magnetite biomineral [13]. Regardless, these nanoparticles are large enough to hold one magnetic field domain and arrangement of magnetosomes in a chain-like structure enables magnetotaxis as a response to the earth's geomagnetic field. Thus, magnetosomes (~25–120 nm) [13, 57] typically exceed the Néel/Brownian transition size (20–25 nm). However, it should be feasible to tailor the synthesis of a magnetosome-like particle [21] such that the biomineral meets the desired size and shape for multispectral MPI. Since current sources of SPION, such as Resovist, have such a spread in size that they reduce MPI sensitivity and spatial resolution, developing a more uniform preparation from a biological source like magnetotactic bacteria would be worthwhile. MPI would benefit significantly if a) SPION of well-defined sizes could be reliably produced and b) the technology could incorporate a reporter gene. Unlike MRI, in which there is potential for development of nonmagnetite-based reporter gene expression, MPI reporter genes must be maghemite- and/or magnetite-based. Hence, preclinical MPI would benefit enormously from the expression of magnetosome-like magnetite nanoparticles and would rival reporter gene applications in preclinical MRI due to the superior sensitivity of MPI, which might be comparable to PET in the future [63]. In addition, MPI, like PET and ^{19}F-MRI [64], is intrinsically quantitative [65]. This is an important advantage over the use of MRI, which becomes problematic when the concentration of SPIO reaches the level of pg/cell [66].

Interestingly, there is evidence in the fossil record that much larger iron biominerals, on the order of 4 μm, were created by biological systems, possibly including eukaryotes [67]. Ortega et al. [68] used PC-12 cells as a model for the dopaminergic neuron in Parkinson's disease (PD) research. These cells differentiate into neurons in response to nerve growth factor. Using an extracellular iron supplement of 300 mM $FeSO_4$ for 24 h and synchrotron technology, they demonstrated that iron was present in 200 nm structures in the cytosol and in neurite outgrowths.

This is consistent with postmortem analysis of the human brain from individuals afflicted with PD, which shows iron in neuromelanin granules [54]. All these reports provide evidence of subcellular iron compartments, quite apart from the traditional ferritin storage. Hence, the real potential of MRI reporter gene expression and generation of sizable iron biominerals for molecular imaging may approach the type of SPIO nanoparticles that have been successfully used to label and track cells by MRI [69].

4 Conclusion

To develop effective reporter gene expression for MRI, the genetic ability of magnetotactic bacteria may be exploited to impart magnetic characteristics to mammalian cells through expression of select magnetosome-related genes. The formation of magnetosome-like nanoparticles in mammalian systems does not necessarily require all the features of the bacterial magnetosome [23, 45]. Based on the success of MagA- and Mms6-derived MR contrast, an imperfect magnetosome-like compartment and/or biomineral may be sufficient, if not desirable, for MRI. Moreover, the stepwise addition of some of the essential magnetosome genes may reconstitute aspects of the magnetosome-like structure that could be associated with changes in cell/tissue contrast and provide unique signatures for MRI reporter gene expression. Employing this type of gene-based MR contrast will not only provide a method for regulating cellular iron biominerals and quantifying the response to transcription factor stimulation, but also enhance the capability of hybrid imaging platforms, such as PET/MRI, and the simultaneous detection of multiple in vivo activities (e.g., edema, hemorrhage, ischemia, inflammation) with anatomical precision. Further development of this medical, molecular imaging tool will enable early characterization of disease progression in both small and large animal models, and forge a path for translation of cell therapies to patient care [70].

Acknowledgments The authors are supported by a grant from the Ontario Research Fund in partnership with Multi-Magnetics Inc., in a grant, entitled Heart Failure: Prevention Through Early Detection Using New Imaging Methods, and by the Cancer Imaging Network of Ontario through Cancer Care Ontario. FSP is the recipient of a Discovery Grant from the Natural Sciences and Engineering Research Council of Canada.

References

1. Bhaumik S, Gambhir S. Optical imaging of Renilla luciferase reporter gene expression in living mice. Proc Natl Acad Sci U S A. 2002;99:377–82.
2. Josserand V, Texier-Nogues I, Huber P, Favrot M-C, Coll J-L. Non-invasive in vivo optical imaging of the lacZ and luc gene expression in mice. Gene Ther. 2007;14:1587–93.
3. Tangney M, Francis K. In vivo optical imaging in gene & cell therapy. Curr Gene Ther. 2012;12:2–11.
4. Couzin-Frankel J. When mice mislead. Science. 2013;342:922–5.

5. Dewald O, Ren G, Duerr G, Zoerlein M, Klemm C, Gersch C, et al. Of mice and dogs: species-specific differences in the inflammatory response following myocardial infarction. Am J Pathol. 2004;164:665–77.
6. Moses W. Fundamental limits of spatial resolution in PET. Nucl Instrum Methods Phys Res A. 2011;648 Suppl 1:S236–40.
7. Thompson K, Wisenberg G, Sykes J, Thompson R. MRI/MRS evaluation of cariporide in a canine long-term model of reperfused ischemic insults. Magnetic resonance imaging/magnetic resonance spectroscopy. J Magn Reson Imaging. 2003;17:136–41.
8. Goldhawk D, Lemaire C, McCreary C, McGirr R, Dhanvantari S, Thompson R, et al. Magnetic resonance imaging of cells overexpressing MagA, an endogenous contrast agent for live cell imaging. Mol Imaging. 2009;8:129–39.
9. Zhang X-Y, Robledo B, Harris S, Hu X. A bacterial gene, mms6, as a new reporter gene for magnetic resonance imaging of mammalian cells. Mol Imaging. 2014;13:1–12.
10. Zurkiya O, Chan AW, Hu X. MagA is sufficient for producing magnetic nanoparticles in mammalian cells, making it an MRI reporter. Magn Reson Med. 2008;59(6):1225–31.
11. Jogler C, Schuler D. Genomics, genetics, and cell biology of magnetosome formation. Annu Rev Microbiol. 2009;63:501–21.
12. Komeili A. Molecular mechanisms of compartmentalization and biomineralization in magnetotactic bacteria. FEMS Microbiol Rev. 2012;36:232–55.
13. Araujo A, Abreu F, Tavares Silva K, Bazylinski D, Lins U. Magnetotactic bacteria as potential sources of bioproducts. Mar Drugs. 2015;13:389–430.
14. Boucher M, Ginet N, Geffroy F, Preveral S, Adryanczyk-Perrier G, Pean M, et al. Genetically functionalized magnetosomes as MRI contrast agent suitable for molecular imaging. International Society for Magnetic Resonance in Medicine (2015) Abstract 0696; Toronto, Canada.
15. Bulte J. In vivo MRI cell tracking: clinical studies. AJR Am J Roentgenol. 2009;193:314–25.
16. de Chickera S, Willert C, Mallet C, Foley R, Foster P, Dekaban G. Cellular MRI as a suitable, sensitive non-invasive modality for correlating in vivo migratory efficiencies of different dendritic cell populations with subsequent immunological outcomes. Int Immunol. 2011;24:29–41.
17. Korchinski D, Taha M, Yang R, Nathoo N, Dunn J. Iron oxide as an MRI contrast agent for cell tracking. Magn Reson Insights. 2015;8(S1):15–29.
18. Nejadnik H, Ye D, Lenkov O, Donig J, Martin J, Castillo R, et al. Magnetic resonance imaging of stem cell apoptosis in arthritic joints with a caspase activatable contrast agent. ACS Nano. 2015;9:1150–60.
19. Matsunaga T, Nakamura C, Burgess J, Sode K. Gene transfer in magnetic bacteria: transposon mutagenesis and cloning of genomic DNA fragments required for magnetosome synthesis. J Bacteriol. 1992;174:2748–53.
20. Nakamura C, Burgess JG, Sode K, Matsunaga T. An iron-regulated gene, *magA*, encoding an iron transport protein of *Magnetospirillum* sp. strain AMB-1. J Biol Chem. 1995;270:28392–6.
21. Stanisland S. Nanoparticle biosynthesis, an accommodating host. Nat Nanotechnol. 2014;9:163–4.
22. Goldhawk D, Gelman N, Sengupta A, Prato F. The interface between iron metabolism and gene-based iron contrast for MRI. Magn Reson Insights. 2015;8(S1):9–14.
23. Goldhawk D, Rohani R, Sengupta A, Gelman N, Prato F. Using the magnetosome to model effective gene-based contrast for magnetic resonance imaging. WIRES Nanomed Nanobiotechnol. 2012;4:378–88.
24. Brennan P, Donev R, Hewamana S. Targeting transcription factors for therapeutic benefit. Mol BioSyst. 2008;4:909–19.
25. Mees C, Nemunaitis J, Senzer N. Transcription factors: their potential as targets for an individualized therapeutic approach to cancer. Cancer Gene Ther. 2009;16:103–12.
26. Corna G, Campana L, Pignatti E, Castiglioni A, Tagliafico E, Bosurgi L, et al. Polarization dictates iron handling by inflammatory and alternatively activated macrophages. Haematologica. 2010;95:1814–22.
27. Fleming R. Hepcidin activation during inflammation: make it STAT. Gastroenterology. 2007;132:447–9.

28. Frangogiannis N. The inflammatory response in myocardial injury, repair, and remodelling. Nat Rev Cardiol. 2014;5:255–65.
29. Nahrendorf M, Pittet M, Swirski F. Monocytes: protagonists of infarct inflammation and repair after myocardial infarction. Circulation. 2010;121:2437–45.
30. Faivre D, Schuler D. Magnetotactic bacteria and magnetosomes. Chem Rev. 2008;108:4875–98.
31. Lohße A, Ullrich S, Katzmann E, Borg S, Wanner G, Richter M, et al. Functional analysis of the magnetosome island in *Magnetospirillum gryphiswaldense*: the *mamAB* operon is sufficient for magnetite biomineralization. PLoS One. 2011;6, e25561.
32. Nudelman H, Zarivach R. Structure prediction of magnetosome-associated proteins. Front Microbiol. 2014;5:article 9.
33. Murat D, Quinlan A, Vali H, Komeili A. Comprehensive genetic dissection of the magnetosome gene island reveals the step-wise assembly of a prokaryotic organelle. Proc Natl Acad Sci USA. 2010;107:5593–8.
34. Hentze M, Muckenthaler M, Galy B, Camaschella C. Two to tango: regulation of mammalian iron metabolism. Cell. 2010;142:24–38.
35. Komeili A, Li Z, Newman DK, Jensen GJ. Magnetosomes are cell membrane invaginations organized by the actin-like protein MamK. Science. 2006;311(5758):242–5.
36. Richter M, Kube M, Bazylinski DA, Lombardot T, Glockner FO, Reinhardt R, et al. Comparative genome analysis of four magnetotactic bacteria reveals a complex set of group-specific genes implicated in magnetosome biomineralization and function. J Bacteriol. 2007;189(13):4899–910.
37. Lefevre C, Trubitsyn D, Abreu F, Kolinko S, Jogler C, Gonzaga Paula de Almeida L, et al. Comparative genomic analysis of magnetotactic bacteria from the Deltaproteobacteria provides new insights into magnetite and greigite magnetosome genes required for magnetotaxis. Environ Microbiol. 2013;15:2712–35.
38. Green S, Komeili A. Biogenesis and subcellular organization of the magnetosome organelles of magnetotactic bacteria. Curr Opin Cell Biol. 2012;24:490–5.
39. Uebe R, Junge K, Henn V, Poxleitner G, Katzmann E, Plitzko J, et al. The cation diffusion facilitator proteins, MamB and MamM of Magnetospirillum gryphiswaldense have distinct and complex functions, and are involved in magnetite biomineralization and magnetosome membrane assembly. Mol Microbiol. 2011;82:818–35.
40. Quinlan A, Murat D, Komeili A. The HtrA/DegP family protease MamE is a bifunctional protein with roles in magnetosome protein localization and magnetite biomineralization. Mol Microbiol. 2011;80:1075–87.
41. Scheffel A, Gardes A, Grunberg K, Wanner G, Schuler D. The major magnetosome proteins MamGFDC are not essential for magnetite biomineralization in Magnetospirillum gryphiswaldense but regulate the size of magnetosome crystals. J Bacteriol. 2008;190(1):377–86.
42. Zeytuni N, Uebe R, Maes M, Davidov G, Baram M, Raschdorf O, et al. Bacterial magnetosome biomineralization—a novel platform to study molecular mechanisms of human CDF-related type-II diabetes. PLoS One. 2014;9:e97154.
43. Rahn-Lee L, Komeili A. The magnetosome model: insights into the mechanisms of bacterial biomineralization. Front Microbiol. 2013;4:352.
44. Geffroy F, et al. In vitro characterization of AMB1 magnetosomes as biogenic functionalized contrast agents dedicated to molecular MRI. World Molecular Imaging Congress (2015) Abstract LBAP 033; Honolulu, USA.
45. Kolinko I, Lohße A, Borg S, Raschdorf O, Jogler C, Tu Q, et al. Biosynthesis of magnetic nanostructures in a foreign organism by transfer of bacterial magnetosome gene clusters. Nat Nanotechnol. 2014;9:193–7.
46. Rohani R, Figueredo R, Bureau Y, Koropatnick J, Foster P, Thompson R, et al. Imaging tumor growth non-invasively using expression of MagA or modified ferritin subunits to augment intracellular contrast for repetitive MRI. Mol Imaging Biol. 2014;16:63–73.

47. Sengupta A, Quiaoit K, Thompson R, Prato F, Gelman N, Goldhawk D. Biophysical features of MagA expression in mammalian cells: implications for MRI contrast. Front Microbiol. 2014;5:29.
48. Lee C, Thompson R, Prato F, Goldhawk D, Gelman N. Investigating the relationship between transverse relaxation rate (R2) and interecho time in MagA-expressing iron-labeled cells. Mol Imaging. 2015;14:551–60.
49. Jensen J, Chandra R. NMR relaxation in tissues with weak magnetic inhomogeneities. Magn Reson Med. 2000;44:144–56.
50. Tanaka M, Mazuyama E, Arakaki A, Matsunaga T. MMS6 protein regulates crystal morphology during nano-sized magnetite biomineralization in vivo. J Biol Chem. 2011;286(8):6386–92.
51. Liu L. Characterization of MagA expression and iron uptake in P19 cells: implications for use as a gene-based contrast agent for MRI. Scholarship@Western electronic thesis and dissertation repository. London, Canada: Western University; 2015.
52. Quiaoit K. Towards the Development of a MagA Reporter gene expression construct for magnetic resonance imaging. Scholarship@Western electronic thesis and dissertation repository. London, Canada: Western University; 2015.
53. Cho I, Moran S, Paudya R, Piotrowska-Nitsche K, Cheng P-H, Zhang X, et al. Longitudinal monitoring of stem cell grafts in vivo using magnetic resonance imaging with inducible *magA* as a genetic reporter. Theranostics. 2014;4:972–89.
54. Collingwood J, Davidson M. The role of iron in neurodegenerative disorders: insights and opportunities with synchrotron light. Front Pharm. 2014;5:191.
55. Andrews N. Anemia of inflammation: the cytokine-hepcidin link. J Clin Invest. 2004;113:1251–3.
56. Wu X-N, Su D, Wang L, Yu F-L. Roles of the hepcidin-ferroportin axis and iron in cancer. Eur J Cancer Prev. 2014;23:122–33.
57. Benoit M, Mayer D, Barak Y, Chen I, Hu W, Cheng Z, et al. Visualizing implanted tumors in mice with magnetic resonance imaging using magnetotactic bacteria. Clin Cancer Res. 2009;15:5170–7.
58. Chen C, Hoult D. Biomedical magnetic resonance technology. Bristol and New York: Adam Hilger; 1989.
59. Liu L, Sengupta A, McGirr R, Thompson R, Prato F, Hoffman L, et al. Expression of the MRI reporter gene *magA* overrides iron export activity in P19 cells. World Molecular Imaging Congress (2015) Abstract LBAP 080; Honolulu, USA.
60. Thorek D, Chen A, Czupryna J, Tsourkas A. Superparamagnetic iron oxide nanoparticle probes for molecular imaging. Ann Biomed Eng [Internet]. 2006.
61. Bauer L, Situ S, Griswold M, Samia A. Magnetic particle imaging tracers: state-of-the-art and future directions. J Phys Chem Lett. 2015;6:2509–17.
62. Rahmer J, Halkola A, Gleich B, Schmale I, Borgert J. First experimental evidence of the feasibility of multi-color magnetic particle imaging. Phys Med Biol. 2015;60:1775–91.
63. Goodwill P, Lu K, Zheng B, Conolly S. An x-space magnetic particle imaging scanner. Rev Sci Instrum. 2012;83:033708.
64. Gaudet J, Ribot E, Chen Y, Gilbert K, Foster P. Tracking the fate of stem cell implants with fluorine-19 MRI. PLoS One. 2015;10:e0118544.
65. Bulte J, Walczak P, Janowski M, Krishnan K, Arami H, Halkola A, et al. Quantitative "hot spot" imaging of transplanted stem cells using superparamagnetic tracers and magnetic particle imaging (MPI). Tomography. 2015;1:91–7.
66. Liu W, Dahnke H, Rahmer J, Jordan E, Frank J. Ultrashort T2* relaxometry for quantitation of highly concentrated superparamagnetic iron oxide (SPIO) nanoparticle labeled cells. Magn Reson Med. 2009;61:761–6.
67. Schumann D, Raub T, Kopp R, Guerquin-Kern J, Wu T, Rouiller I, et al. Gigantism in unique biogenic magnetite at the paleocene-eocene thermal maximum. Proc Natl Acad Sci U S A. 2008;105:17648–53.
68. Ortega R, Cloetens P, Deves G, Carmona A, Bohic S. Iron storage within dopamine neurovesicles revealed by chemical nano-imaging. PLoS One. 2007;2:e925.

69. Graham J, Foltz W, Vaags A, Ward M, Yang Y, Connelly K, et al. Long-term tracking of bone marrow progenitor cells following intracoronary injection post-myocardial infarction in swine using MRI. Am J Physiol Heart Circ Physiol. 2010;299:H125–33.
70. Xu H, Belkacemi L, Jog M, Parrent A, Hebb M. Neurotrophic factor expression in expandable cell populations from brain samples in living patients with Parkinson's disease. FASEB J. 2013;27:4157–68.
71. Meikle S, Kench P, Kassiou M, Banati R. Small animal SPECT and its place in the matrix of molecular imaging technologies. Phys Med Biol. 2005;50:R45–61.
72. Cherry S, Sorenson J, Phelps M. Single photon emission computed tomography. Physics in nuclear medicine. 3rd ed., 2003. p. 299–324.
73. Chen B, Legant W, Wang K. Lattice light-sheet microscopy: imaging molecules to embryos at high spatiotemporal resolution. Science. 2014;346:1257998.
74. Ephrat P, Albert G, Roumeliotis M, Belton M, Prato F, Carson J. Localization of spherical lesions in tumor-mimicking phantoms by 3D sparse array photoacoustic imaging. Med Phys. 2010;37:1619–28.
75. James M, Gambhir S. A molecular imaging primer: modalities, imaging agents, and applications. Physiol Rev. 2012;92:897–965.
76. Gore J, Yankeelov T, Peterson T, Avison M. Molecular imaging without radiopharmaceuticals? J Nucl Med. 2009;50:999–1007.